IOPscience iopscience.iop.org

Home Search Collections Journals About Contact us My IOPscience

Metastability and disorder effects in nonstoichiometric VS_2

This article has been downloaded from IOPscience. Please scroll down to see the full text article.

2002 J. Phys.: Condens. Matter 14 2677

(http://iopscience.iop.org/0953-8984/14/10/317)

View the table of contents for this issue, or go to the journal homepage for more

Download details:
IP Address: 171.66.16.27
The article was downloaded on 17/05/2010 at 06:18

Please note that terms and conditions apply.

INSTITUTE OF PHYSICS PUBLISHING JOURNAL OF PHYSICS: CONDENSED MATTER

J. Phys.: Condens. Matter **14** (2002) 2677–2689 PII: S0953-8984(02)32391-9

Metastability and disorder effects in nonstoichiometric VS_2

P Poddar[1,2] **and A K Rastogi**

School of Physical Sciences, Jawaharlal Nehru University, New Delhi-110067, India

E-mail: ppoddar@post.tau.ac.il

Received 7 January 2002
Published 18 March 2002
Online at stacks.iop.org/JPhysCM/14/2677

Abstract

In this detailed study we have reported on single-crystal and polycrystalline phases of $V_{1+x}S_2$; $0.10 < x < 0.25$, prepared using excess sulfur in a sealed quartz tube and investigated their structural, transport and magnetic properties. The crystal flakes have trigonal symmetry with $2c$ and incommensurate $>2(\sqrt{3})a$ superlattice ordering in the a–b plane. As-grown flakes showed complex irreversible behaviour in resistivity on cycling to low temperatures, related to the metastability of the structure. The annealing of the crystal flakes and addition of 5–10% Al stabilizes the superstructure. We observe an anomalous contribution to the resistance of these crystal flakes with a maximum around 100–150 K. The contribution is more pronounced for better-ordered phases. The magnetic susceptibility and thermopower values of these compounds are large and vary smoothly on cooling around this temperature interval. The polycrystalline phase, obtained at a higher temperature, on the other hand, showed absence of superlattice distortions and gave a smooth behaviour in its resistance, but with a large T^2-contribution. The structural and electronic properties of different phases are discussed in terms of disorder among the interstitial V atoms and the effect of in-plane vacancies on the charge-density-wave instability in these and similar compounds.

1. Introduction

In the family of early transition metal chalcogenides, the relatively ionic compounds like VS_2, CrS_2 and $CrSe_2$ are known to have metastable layered structure. The high-temperature synthesis of these compounds produces cation-rich compositions, in which the interstitial atoms in the van der Waals gap of the layers provide structural stability. The ideal layer structures of these compounds have been prepared at room temperature by the indirect route of de-intercalation of

[1] Author to whom any correspondence should be addressed.
[2] Present address: School of Chemistry, Tel Aviv University, Tel Aviv-69978, Israel.

 © 2002 IOP Publishing Ltd Printed in the UK

$LiVS_2$ and $KCrSe_2$, using topotactic oxidation by I_2 in an acetonitrile solution [1,2]. In cation-rich compositions the ordering of the interstitial cations and ensuing structural distortions provide further stability for phases having compositions between VX_2 and VX: X = S, Se or Te.

In V_5S_8, V_3S_4 and VS the structural distortions are accompanied by considerable shifting of metal atoms from ideal octahedral sites, to form strong in-plane and interplane intermetallic bonds. This tendency to cluster is also found in ternary compositions such as $BaVS_3$ and GaV_4S_8, giving respectively well-separated V chains and tetrahedral V_4 clusters [3, 4]. Interestingly, in Cr compounds, similar clustering is not found. The intermediate bonding character of the valence electrons of vanadium in these cluster compounds gives rise to some remarkable electronic properties [5]. The d-band stabilization by metal clustering also gives rise to a highly anisotropic thermal expansion behaviour over large temperature intervals in 1T-CrS_2 and 1T-VS_2 and also in V_5S_8 and VS [6].

The range of stoichiometry of the different vanadium sulphide phases is quite broad [7]. The synthesized compositions are a function of temperature as well as of starting material. A detailed study of off-stoichiometry of Ti and V monosulphides and selenides and their mixed compositions has been made by Henderson and Goodenough [8]. It was noted that the stability of the NiAs-type ideal hexagonal structure of these phases critically depends on cation or anion defects, which influence the valence electron concentration. The stabilization of narrow bands of 3d orbitals is achieved through metal clustering, reduction of c/a ratio and/or magnetic ordering. The transport properties are also greatly influenced by localized, itinerant or trapped electron behaviour in metallic clusters [5, 8].

1.1. Sulphur-rich compositions of V–S

As mentioned above, near-ideal CdI_2-type layered VS_2 with a large c/a ratio of 1.788 could be prepared at room temperature by the indirect route of using $LiVS_2$, and is reported to be chemically stable only up to 300 °C. A transition in magnetic susceptibility around 305 K was observed, which was attributed to CDW instability, mainly because of its large c/a ratio as in Nb and Ta dichalcogenides [1]. The correct nature of this transition could not be ascertained because of the absence of any superlattice distortions in the x-ray diffraction and the lack of conductivity measurements. Moreover, the stronger e–e interactions in sulphides might have been expected to suppress the CDW transition to lower temperature than that (110 K) observed for VSe_2 [9].

The most sulfur-rich composition prepared by the reaction of elements at 800 °C is V_5S_8, which has been extensively studied [10–14]. In this compound, the extra 25% of V atoms occupy ordered positions in a monoclinically distorted structure between the filled layers of VS_2. The interactions among V atoms give four-atom clusters in the filled layers and these are connected to neighbouring layers by interlayer vanadium [10]. In addition, an anomalously large a-axis contraction due to progressive increase in V–V bonding is observed on cooling down to 100 K [15]. Simultaneously, the Hall coefficient shows a changeover from predominantly p-type to n-type conduction on cooling [11]. The magnetic susceptibility is strongly temperature dependent and it shows an itinerant-type antiferromagnetic transition below $T_N = 32$ K. The details of the magnetic properties are controversial [13, 14].

The next V-rich phase showing ordered-vacancy structure is V_3S_4. Here V–V zigzag chains run along c-direction in an orthorhombically distorted structure. The magnetic susceptibility, although highly enhanced, is nearly temperature independent. An itinerant antiferromagnetic transition below 8 K is reported for V_3S_4 [14].

A nonstoichiometric phase, $V_{1+x}S_2$ with $x = 0.1$, was synthesized by the decomposition of VS_4 at 800 °C under 20 kbar pressure [16]. The structure was found to be similar to 1T-

VS_2, but with random vacancies (16%) in the otherwise filled layers. The interlayer V atoms (20%) also have a disordered arrangement. The c/a ratio of 1.738 is considerably smaller than the 1.788 of the metastable VS_2. The electronic properties of this phase are not known. A reversible vacancy order–disorder transition above 800 °C in the single crystals of V_5S_8 has also been reported [17]. At higher temperatures, the intralayer vacancies in every second layer are disordered, while the interlayer ordering is only partially changed. A metastable composition $V_{1.2}S_2$ with trigonal symmetry was found by quenching the sulfur-rich VS_2 composition from 600 °C to room temperature. On reheating to 450 °C, this phase converts to stable V_5S_8 (see the second reference of [7]).

The above discussion suggests a crucial role of interlayer vanadium atoms in the structural stability of $V_{1+x}S_2$ compositions. We have grown single-crystal flakes of nominal compositions $V_{1+x}S_2$ and Al_xVS_2 with $x \leqslant 0.2$, using excess sulfur in a sealed quartz tube. In the following sections we present their structural, transport and magnetic properties.

2. Sample preparation

Single crystals were prepared by vapour transport in a sealed quartz tube placed in a horizontal temperature gradient. For binary phases a total of 2 g of the elements, V 2N7 and S 5N, were sealed in 1:2.1 molar ratio in a 12 cm long, 1 cm diameter quartz tube. After prolonged reaction at lower temperatures, the charge was maintained at 600 °C while other end was maintained at 700 °C for about a week. Large numbers of plate-like crystals, 5–7 mm in size and 50–100 μm thick, were obtained near the colder end where the temperature varied from 620 to 640 °C. Inductive coil plasma (ICP) analysis showed that the crystals have an average stoichiometry of $V_{1.2}S_2$. In another attempt, the reacted charge was held in a vertical position at 750 °C for three weeks. In this case, only a compact of coarse grain crystallites was obtained without any transport of material. The structural and transport properties of this phase are different from those of the crystal flakes, as will be discussed below. For ternary phases, 5–10%Al (5N filings) was added to V and S. In this case, the mixture was heated to 800 °C for the complete reaction of Al. The crystals were also obtained by adding about 0.05 mmol cm^{-3} of iodine in the sample tube. The tube was put in a horizontal position with the charge at a higher temperature of 850 °C. The crystals were obtained at the colder end, maintained at 750 °C.

3. Structure

A preliminary investigation of the crystal structure of these compounds was made by means of x-ray diffraction at room temperature, on finely ground crystals, using Cu Kα radiation, after carefully minimizing orientation effects. It is worthwhile to compare these patterns with that of a compound, V_5S_8, for which a detailed study has been reported by other workers [7, 10]. V_5S_8 belongs to monoclinic system with space group $F2/m$–C_{2h}^3, a derivative group of hexagonal 1T-VS_2 ($P3m1$). The monoclinic cell dimensions are related to the hexagonal cell by $a_m \leqslant 2(\sqrt{3})a_h$, $b_m > 2a_h$, $c_m = 2c_h$ and $\beta = 91.5°$. In figure 1(e), we have presented the pattern expected for V_5S_8, using atomic positions given by De Vries and Jellinek [7]. However, in order to compare it with patterns for our compounds, we have indexed the peaks on the basis of an undistorted hexagonal cell using $2a_h \times 2c_h$, with $a_h = 3.27$ Å and $c_h = 5.66$ Å, and ignoring the splitting due to its actual reduced symmetry.

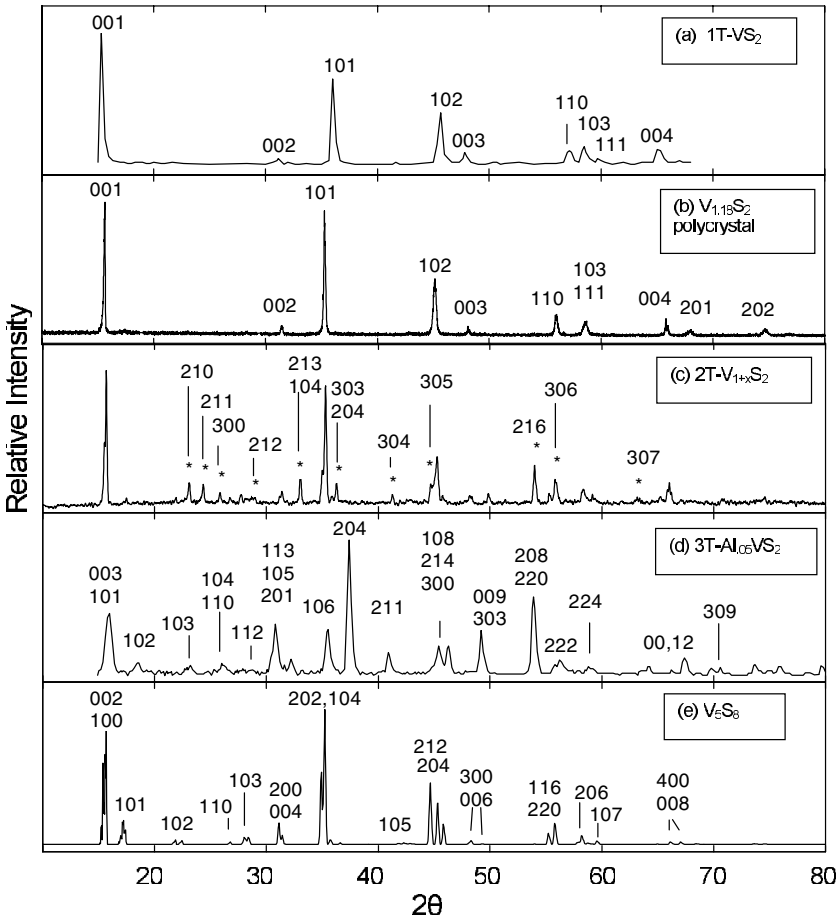

Figure 1. XRD patterns of: (*a*) 1T-VS_2 prepared by de-intercalation of $LiVS_2$ [1], (*b*) polycrystalline $V_{1.18}S_2$ obtained at 750 °C, (*c*) crystal flakes with excess S at 650 °C, giving a two-layer structure and superstructure lines marked by asterisks (see the text), (*d*) the three-layer structure of $Al_{0.05}VS_2$; and (*e*) the pattern generated through General Structure Analysis System Software using the parameters of V_5S_8 [7] and indexed on a $2a \times 2c$ hexagonal cell.

3.1. $V_{1+x}S_2$ crystal flakes

The self-intercalation of excess V atoms between the layers results in marked changes in the structure of $V_{1+x}S_2$. Firstly, as presented in table 1, the c/a ratio reduces from 1.788 for pure 1T-VS_2 to 1.72. The cell parameters are now quite similar to those of other metal-rich phases including V_5S_8. Secondly, there are large numbers of additional lines, marked in figure 1(*c*) by asterisks, which are absent for $V_{1.18}S_2$ (polycrystalline) as well as for monoclinic V_5S_8. We were able to index these lines on a $2(\sqrt{3})a_h \times 2c_h$ superlattice, but with a value of a_h ($\approx$3.40 Å) larger than that calculated for the main lines. This indicates incommensurate distortion of the trigonal cell in single crystals and should be compared with ordered-vacancy monoclinic V_5S_8. A detailed study of the single-crystal XRD will be required to reveal the true nature of the incommensuration. At present we just note that apart from a superlattice distortion, $V_{1+x}S_2$ crystals obtained at a lower temperature retain trigonal symmetry, as for the disordered-vacancy $V_{1.1}S_2$ and $V_{1.2}S_2$ phases prepared at high pressure by Nakano-Onada *et al* [16] and reported as being obtained by Jellinek on quenching a sulfur-rich composition [18].

Table 1. Structural details for different compounds.

Compound	Preparation details	Layers	Lattice constants a (Å)	c (Å)	c/a[a]	Transition temperature (K)
VS_2[b]	De-intercalation of $LiVS_2$	1T	3.22	5.76	1.79	310 K, CDW
$V_{1.1}S_2$[c]	VS_4 decomposition at high pressure	1T	3.27	5.69	1.74	—
$V_{1+x}S_2$[d]	Crystal at 650 °C	2T	3.29 $2(\sqrt{3}) \times 3.40$	5.66 2×5.66	1.72 —	Metastable, 100 K (annealed)
$V_{1.18}S_2$	Polycrystalline 750 °C for three weeks	1T	3.28	5.67	1.73	—
V_5S_8[e]	Crystals at 850 °C	Two-layer monoclinic	$2(\sqrt{3}) \times 3.27$ 2×3.32	2×5.66 $\beta = 91.5°$	1.73–1.70	Antiferromagnetic 32 K
$Al_{0.05}VS_2$	Crystals at 750 °C	3T	2×3.40	3×5.56	1.63	120 K
$Al_{0.05}VS_2$	Polycrystalline at 850 °C	2T	2×3.29	2×5.6	1.72	—

[a] c/a calculated for single layer.
[b] Reference [1].
[c] Reference [16].
[d] Showing superlattice distortion (see the text).
[e] References [7, 10].

In spite of the trigonal symmetry, the similarity of its supercell dimensions with those of monoclinic V_5S_8 strongly suggests the presence of in-plane V-atom clusters in the crystal flakes of $V_{1+x}S_2$ and only partially ordered V atoms in the van der Waals gap. In the latter, the interlinking of clusters along the c-direction would be significantly affected by the interstitial-atom disorder. Depending upon the preparation conditions and nature of the vacancy disorder, various metastable configurations of clusters are then expected. These structural features seem to be the reason for the instability of the as-grown $V_{1+x}S_2$ flakes and the observed irreversibility in the resistivity on temperature cycling.

3.2. Polycrystalline $V_{1.18}S_2$

The higher-temperature synthesis gave a polycrystalline phase. The XRD pattern reported in figure 1(*b*) reveals complete absence of the superlattice lines observed for the flakes in figure 1(*c*). The sharp lines for this phase could be indexed with half the cell constants ($a = 3.28$ Å, $c = 5.57$ Å) of the flakes. Although the XRD pattern is now quite similar to that for the stoichiometric compound VS_2, its c/a ratio of 1.729 is nearly same as for the other $V_{1+x}S_2$ compounds (see table 1). The complete absence of superstructural lines shows that the high-temperature treatment leads to a homogeneously disordered arrangement of interstitial atoms, which probably also eliminates the V-atom clustering among intralayer atoms. The transport properties of the polycrystalline phase, presented below, show complete reversibility on temperature cycling and a stable structure, in contrast to the crystal flakes.

3.3. Al_xVS_2, $x \leqslant 0.1$

We also obtained the crystal flakes after adding 5 and 10% Al and using I_2-vapour transport at a higher temperature (of 750 °C) than for $V_{1+x}S_2$. The untransported charge left at 850 °C gave exactly the same x-ray pattern as V_5S_8. The crystals, on the other hand, gave quite a different pattern, reported in figure 1(*d*), with the strongest lines at 37.2° and 54°. The pattern

could be indexed on the basis of a three-layer structure, along with a considerable reduction in c/a ratio to the value for the close packing of layers. The presence of 103 and 106 lines upon using a hexagonal $2a \times 3c$ cell, however, rules out the simple 3R lattice which is quite common among the metal-rich sulphides and selenides of V and Cr. Moreover, the individual lines of these crystal flakes are considerably broadened, indicating a substantial spread in the distortion factor. It is worthwhile to mention here that the polytypic two-layer CdI_2-type and three-layer $CdCl_2$-type structure modifications are also obtained in the ternary chalcogenides of V with alkali metals [19]. The strong reduction in the c-parameter for this phase is due to the stronger interplane metal–atom interactions caused by the extra electrons from aluminium atoms.

4. Electronic properties

The electrical conductivity of the crystal flakes was measured using silver paint contacts in van der Pauw geometry. Because of the small size and irregular thickness (50–70 μm), the calculated resistivity values are correct only to within 50%. All the crystal flakes showed strong resistance variations during the initial evacuation process and for slight heating of specimen. Stable values were, however, obtained at room temperature after adequate pumping. In order to avoid reaction with the silver contacts via Joule heating, the measurements were done using small currents $\leqslant 100$ μA, The thermoelectric power was measured with respect to Cu. The absolute value was obtained after subtracting the contribution of the connecting leads. This contribution was obtained by making a separate measurement on pure lead under the same conditions and using its absolute value from the literature. The magnetic susceptibility was measured for randomly oriented crystals between 90 and 350 K in a field of 0.8 T by using a vibrating-sample magnetometer (VSM).

4.1. Metastability in $V_{1+x}S_2$ flakes

The as-grown crystals of $V_{1+x}S_2$ showed varied and complex resistivity behaviour on cooling. The typical behaviour of occasional jumps to higher values and a large irreversibility on temperature cycling is shown in figure 2 for one of the virgin flakes (figure 2(a), $\rho_{300} \sim 500$ $\mu\Omega$ cm). The repeated cycling to low temperatures increased the overall resistance and gave a sharp jump (figure 2(b)) to a higher value on cooling below 200 K. In the low-temperature phase the hysteresis is reduced, but a clear resistance minimum is noticed at 20 K. For some of the more metallic flakes (not reported here) the resistance showed no hysteresis, but we saw a shallow resistance minimum around 100–150 K. We believe that these different behaviours of the resistivities of flakes are due to different stoichiometries and differences in the short-range order of the vanadium atoms. The isothermal measurement of the resistance after rapid quenching did not indicate any relaxation effects.

In figure 3, we report the resistance behaviour of another flake after annealing it at 500 °C. A resistance anomaly at 100 K is preceded by a small hysteresis at high temperature. The superlinear behaviour at higher temperature and a nearly linear drop below 100 K are qualitatively similar to the behaviours reported for layer chalcogenides of Nb, Ta and VSe_2, undergoing CDW-coupled periodic lattice distortions (PLD). The detailed behaviour near incommensurate–discommensurate–commensurate transitions depends sensitively upon the lattice defects, especially in the case of the more ionic sulphides. We should also recall that the superlattice reflections in the crystal flakes are incommensurate at room temperature and that the excess V atoms are expected to have only a short-range order. The different behaviour below 100 K after annealing of the flakes seems to be due to increase in the atomic order and the commensuration of the CDW below about 100 K. In contrast to the crystal flakes,

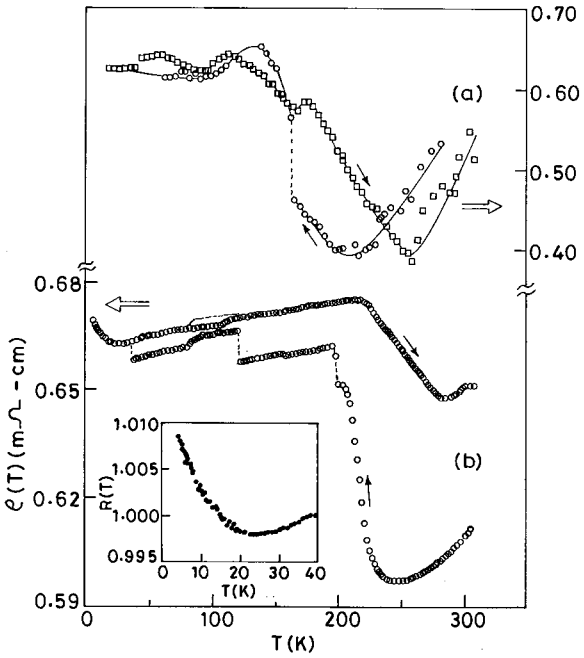

Figure 2. Irreversible conduction behaviour of as-grown $V_{1+x}S_2$ flakes. The curves labelled (*b*) were obtained after repeated cooling.

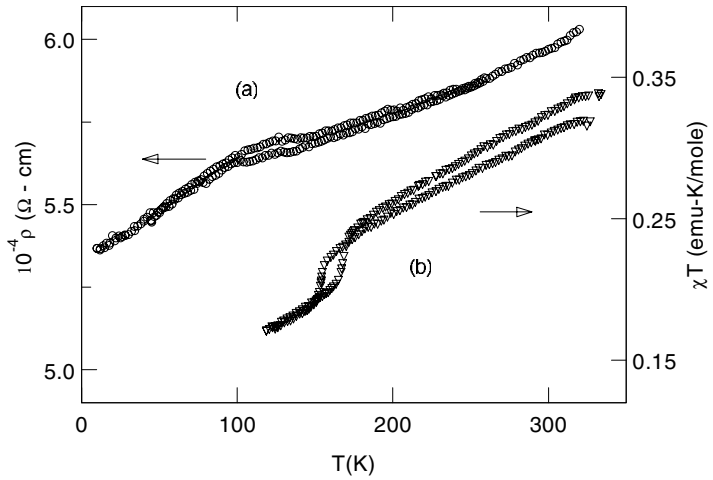

Figure 3. (*a*) The resistance of annealed $V_{1+x}S_2$ flakes showing small hysteresis on cooling and a kink around 100 K. (*b*) The magnetic susceptibility of randomly oriented crystal flakes plotted as χT versus T. The origin of the 170–200 K anomaly in χ is not known.

the high-temperature phase of $V_{1.18}S_2$, reported on below, showed complete suppression of the lattice distortion and the anomaly in resistivity because of the increased disorder of the V atoms.

In figure 3, we have also shown the magnetic susceptibility results on a randomly oriented mass of crystal flakes. The results are plotted as χT versus T. The linearity of the plot, the

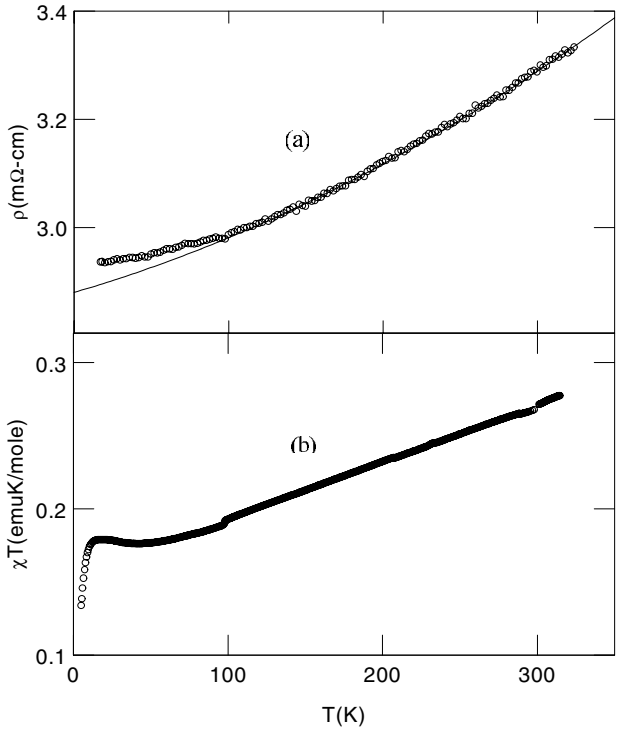

Figure 4. Resistivity and magnetic susceptibility presented as χT versus T for polycrystalline $V_{1.18}S_2$. The continuous curve is $\rho(T) = \rho_0 + AT + BT^2$.

hysteresis at high temperature and an anomaly below 170 K can be noted. The sharp drop in χ below 200 K does not seem to be directly related to the anomaly at a lower temperature of 120 K in the resistivity of the annealed phase. A detailed correlation of this anomaly with the irreversibility in the transport properties discussed above cannot at present be achieved, since the electronic transport in the plane of individual flakes is expected to be extremely sensitive to the inhomogeneity of the chemical composition and to the short-range disorder. In contrast, the magnetic susceptibility measurements give bulk-averaged properties of the crystal flakes and seem to be rather insensitive to the nature of the short-range atomic correlations.

4.2. Disordered $V_{1.18}S_2$

The crystal structure of the polycrystalline mass obtained at a high temperature was found to be same as that of 1T-VS_2, wherein the interplane vacancies and the disorder among V sites led to complete suppression of the lattice distortion. The compact mass of tiny crystallites was cut into rectangular pieces for four-probe resistance measurements. The resistivity and the magnetic susceptibility results are presented as figures 4(*a*) and 4(*b*) respectively.

The resistivity at room temperature is considerably higher than that of the flakes, but it is not clear whether there is a large contribution from intergrain resistance or whether the increase is related to the V-atom disorder. In any case, there does not seem to be the apparent anomaly on cooling found for the flakes. The curve is also highly reproducible on temperature cycling. It closely follows a $\rho(T) = \rho_0 + AT + BT^2$ dependence, shown in the figure by a continuous line. Here ρ_0, A and B are respectively the resistance due to static disorder, the linear coefficient due to e–ph scattering and the coefficient of the quadratic temperature

Table 2. Magnetic susceptibility parameters obtained at high temperatures (100–300 ∼ K), shown as $\chi = \chi_0 + (C/T)$. All compounds are polycrystalline except where otherwise stated.

		Parameters		
Compounds	$\chi(300)$ (10^{-4} emu/(g atom V))	χ_0 (10^{-4} emu/(g atom V))	C_m (emu K/(g atom V))	Comments
1T-VS_2	1.5	2.53 ($T > 310$ K) 1.5 ($T < 310$ K)	—	Transition at 310 K [1]
	4.5	4.3 ($T > 110$ K)	0.006	CDW onset
1T-VSe_2		3.6 ($T < 50$ K)		at 110 K [20]
V_5S_8	8.4	3.7	0.133	$\theta_{cw} = +23$ K $T_N = 32$ K [25]
2T-$V_{1+x}S_2$	9.7	5.7 ($T > 150$ K) 5.2 ($T < 150$ K)	0.126 0.10	Transition at 150 K
1T-$V_{1.18}S_2$	7.63	3.3	0.13	Polycrystalline
3T-$Al_{.05}VS_2$	8.3	2.9	0.16	Crystal flakes
3T-$Al_{.10}VS_2$	7.7	2.6	0.15	Crystal flakes

dependence for e–e scattering. However, a small deviation is seen below 100 K where the crystal flakes reported on above showed sharp anomalies in $R(T)$.

In common with the other metallic compounds of the vanadium, $V_{1+x}S_2$ shows a magnetic susceptibility that is strongly temperature dependent. We have plotted it as χT versus T, in order to show the temperature-independent χ_0 and Curie contribution. These parameters are noted in table 2. It is interesting to compare the magnetic property of our compounds with those of the much-studied V_5S_8, showing an itinerant antiferromagnetic transition below 32 K [7–9, 17, 18]. The existence of the T^2-term in the resistivity and a large χ_0-term clearly suggests a narrow band in our compounds. The clear deviation seen in χ below 50 K in figure 4 may be related to the strong-correlation effects in this narrow-band material.

4.3. Al_xVS_2

The addition of 5–10% Al to VS_2 also produced crystal flakes at higher temperature (750 °C). As already mentioned, the XRD pattern however indicates a three-layer structure and reduced c/a ratio for the crystal flakes, but with similar in-plane superstructural distortion as in the aluminium-free composition. The absence of irreversible $R(T)$ behaviour suggests a stable structure for these phases. In figure 5, we present the room temperature normalized resistance behaviour of these compounds. The low-temperature residual resistance is quite high, with $R_{300}/R_{4.2} \approx 1.1$–$1.2$ measured for different flakes. Here again we observe an anomalous temperature dependence on cooling below room temperature, as for the annealed flakes of $V_{1+x}S_2$ reported on in figure 3. A point of inflection in $R(T)$ at 150 K for 5% Al and at 130 K for 10% Al flakes can be noted. In the inset, we show typical resistance minima observed at 15–20 K. The qualitative similarity of the resistivity behaviour to that of the low-temperature-annealed $V_{1+x}S_2$ flakes and the absence of the irreversibility found for as-grown flakes indicates the stability of the structure on Al addition. This suggests a defect-stabilized structure for the nonstoichiometric compositions of VS_2.

In figure 5(*b*), we have reported the magnetic χ-results for Al_xVS_2. The χT–T plots are linear and give a smooth and reversible behaviour, in contrast to that for the as-grown metastable flakes $V_{1+x}S_2$ reported in figure 3. Also the absence of a corresponding anomaly in χ around 150–130 K in the stable phases, including the annealed $V_{1+x}S_2$, suggests that the

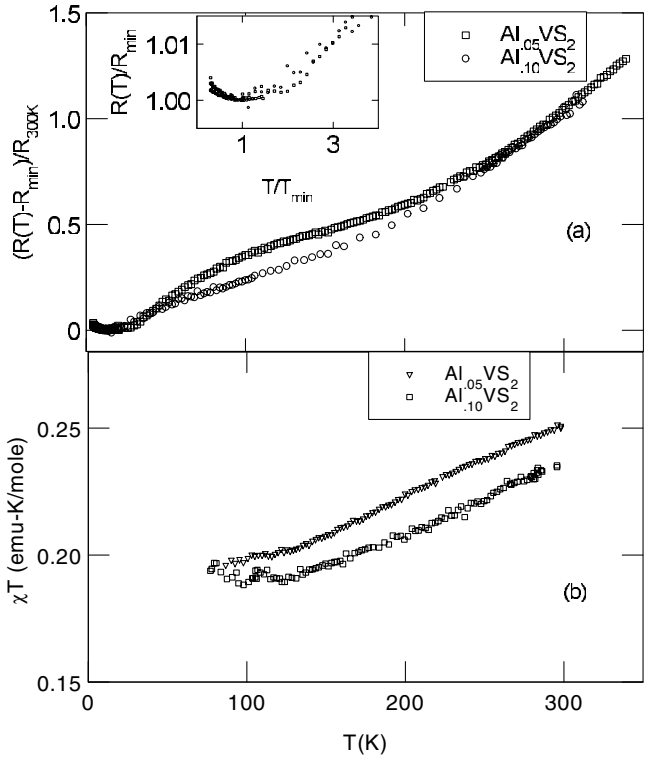

Figure 5. (*a*) Normalized resistance $(R(T) - R_{min})/R_{300}$ curves for Al_xVS_2 flakes. The resistance minimum behaviour is shown in the inset, at $T_{min} = 15$ and 20 K respectively for $x = 0.05$ and $x = 0.1$ Al. (*b*) Magnetic susceptibility plotted as χT versus T for randomly oriented Al_xVS_2-flakes.

magnetic properties are not significantly affected at the transition observed in the resistivity of these compounds.

A small addition of aluminium results in χ being similar to that of VS_2 but with an additional temperature-dependent contribution, most probably from the electrons localized on extra interstitial vanadium atoms, which are not present in VS_2. If we associate $\sim 2.5\ \mu_B$/interstitial atom, as reported for the d^2 configuration of interstitial V atoms in VSe_2, then the observed Curie constant would correspond to about 12–20% of the interstitial V atoms in these compounds. The relatively large value of χ for all of these compounds can be related to narrow bands due to superlattice distortion, which gives separated clusters of in-plane vanadium.

4.4. Thermopower

The thermopower measurements were done on sintered pellets of Al_xVS_2 and on one of the $V_{1+x}S_2$ crystal flakes along its plane. The temperature dependence of the absolute Seebeck coefficient is shown in figure 6. The room temperature values are positive. Although the overall temperature dependence is metal-like, the saturation effects for the in-plane thermopower of $V_{1+x}S_2$ at high temperatures and a rapid drop to negative values, especially for the pellets at lower temperatures, can be noticed. This changeover is frequently observed in semimetallic group V and VI transition metal chalcogenides near structural distortions,

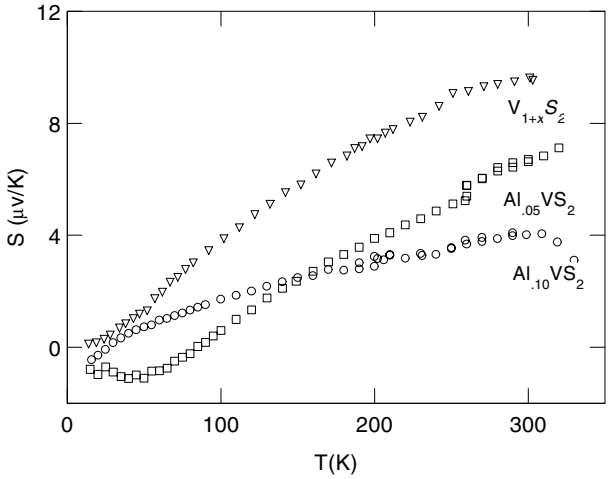

Figure 6. The absolute thermopower across the plane for $V_{1+x}S_2$ flakes and Al_xVS_2 pellets.

where at the Fermi surface the effects of the hybridization of nonbonding d bands with the chalcogen valence band continuously change. In view of the complicated metallic sublattice structure and localized spin fluctuations in these compounds, which would strongly affect the electron scattering and its energy dependence, a clear explanation of the observed thermopower behaviour cannot be provided. As for the crystal flakes, for $\chi(T)$ the $S(T)$ dependence also gave a smooth variation, without any noticeable anomalies around 100–150 K. This suggests that, unlike the electrical transport, the thermal diffusion of charge carriers, which contributes to the thermopower, is not much affected by the structural relaxation on cooling.

5. Discussion

The structural transport and magnetic properties of nonstoichiometric phases of $V_{1+x}S_2$, $x \leqslant 0.2$, are quite complex. These phases contain excess V atoms in between the layers of 1T-VS_2. An interesting aspect of the structure reported in this study is the noncommensurate $2(\sqrt{3})a \times 2c$ superlattice distortion for the crystal flakes grown in excess sulfur. The transport properties of as-grown flakes are highly complex and show sharp jumps and large irreversibility on cooling, related to the metastability of the structure. The structure can be stabilized by two different methods: low-temperature annealing of the flakes and addition of Al at a higher temperature. These methods both reveal an electronic instability on cooling below room temperature due to additional distortions of the lattice followed by a weak transition around 100–130 K. The magnetic χ and the thermopower gave smooth but strongly temperature-dependent behaviour.

In contrast to the above-mentioned flakes, the polycrystalline $V_{1.18}S_2$ synthesized at high temperature had a basic 1T-VS_2 structure which is stabilized by large in-plane V-atom vacancies and homogeneously disordered interstitial atoms, as reported by other workers [16, 17]. The in-plane V-atom vacancies remove the superlattice distortions and the conductivity follows a smooth reversible metallic behaviour down to 15 K. A large T^2-term in the resistivity and a large temperature-dependent magnetic susceptibility clearly indicate narrow energy bands and highly correlated electrons in these compounds.

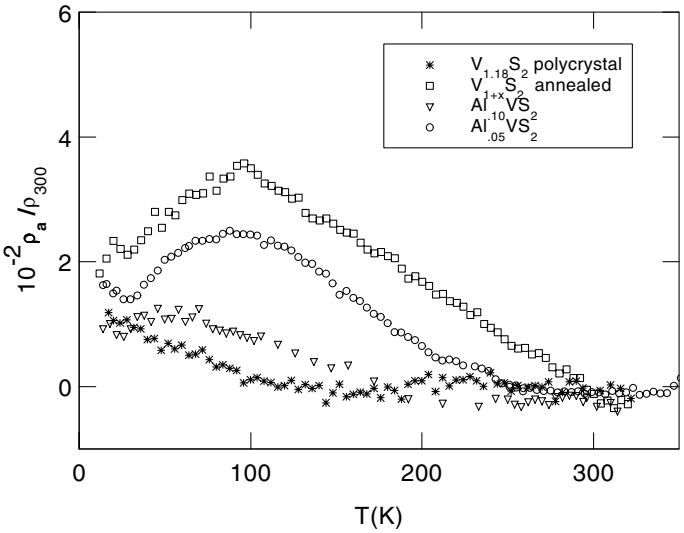

Figure 7. The additional contribution to the resistance for different compounds, ρ_a/ρ_{300}, obtained after subtracting the normalized resistance of polycrystalline $V_{1.18}S_2$, which follows $\rho = \rho_0 + AT + BT^2$, as shown in figure 4(*a*).

In figure 7, we have plotted the additional resistance normalized to the room temperature value, ρ_a/ρ_{300}, associated with the resistance anomaly in different phases. This contribution was calculated after subtracting the properly normalized resistance of completely disordered $V_{1+x}S_2$, which showed a $\rho = \rho_0 + AT + BT^2$ dependence above 100 K. The additional contribution in the resistance is clearly largest for binary $V_{1+x}S_2$ flakes, which were annealed at 500 °C. They have maximum short-range order, as indicated by sharp superlattice lines in the XRD patterns. The reduced contribution to the resistance of Al-containing phases is probably due to in-plane V vacancies created by the high-temperature synthesis of the phases.

In this investigation, it has not been possible to establish a definite cause of the anomaly in the resistance—since incommensurately modulated structures are also observed in such diverse systems as the metallic alloys CuSb and the insulating ordered-vacancy phases VO_x, TiO_x and V_nC_{n-1}. Nevertheless, we note the similarity with 1T-VSe_2 as regards the resistance behaviour and the effect of disorder below 110 K [20], in which the lattice distortion is related to the formation of CDWs. The resistivity shows a maximum below the onset temperature. Similarly, for pure 1T-VS_2, a sharp anomaly in $\chi(T)$ at 305 K has been inconclusively related to CDW formation [1]. The absence of a superlattice in our polycrystalline $V_{1.18}S_2$, on the other hand, can be similarly related to the fast suppression of CDWs observed in ion-irradiated VSe_2, creating in-plane V vacancies [20]. As can be seen in figures 4(*a*) and 7, for the Al-stabilized phases there is an additional upturn below 15–20 K. The high resistivity and the resistance ratio $R_{300}/R_{4.2}$ of only 1.1–1.2 clearly show that in these phases the disorder is considerably higher and, in the presence of the strong e–e interaction, weak localization, as proposed by Althshuler and Aronov [21], is observed. Similar electron localization effects were previously reported in Ga-intercalated NbS_2 [22].

The nonstoichiometric and intermediate disorder in the compounds in the present study should significantly affect the band structures and hence the CDW transitions reported for similar layered compounds. Moreover, the extremely enhanced electronic correlations effects

in our $V_{1+x}S_2$, which are comparable to those in antiferromagnetic V_5S_8, may well lead to the suppression of a CDW state to give a SDW as proposed by Wilson *et al* [23]. This, however, does not seem to be the case, as can be concluded from our magnetic susceptibility results. It should also be noted that different band-structure calculations [24] gave largely similar band energies for isostructural VS_2 and VSe_2. This is because increased hybridization with chalcogens compensates for the larger intermetallic distances between V atoms in selenides. Moreover, the Fermi surface topology of sulphides, being more two dimensional, is more favourable to CDW stability. A comprehensive theoretical study is therefore required in order to understand the electronic transition observed in these narrow-band materials.

Acknowledgments

The powder XRD investigation was done at the School of Environmental Science, Jawaharlal Nehru University, and the Solid State Physics Laboratory, New Delhi. The magnetic susceptibility measurement on one of the samples was done in TIFR, Mumbai. One of us (Pankaj Poddar) thanks the University Grant Commission, India, for financial support. We acknowledge the critical suggestions from Professor Deepak Kumar, SPS, JNU, made during the preparation of this paper.

References

[1] Murphy D W, Cross C, DiSalvo F J and Waszczak J V 1977 *Inorg. Chem.* **16** 3027
[2] Fang C M, van Bruggen C F, de Groot R A, Weigers G A and Haas C 1997 *J. Phys.: Condens. Matter* **9** 10 173
[3] Nakamura M, Sekiyama A, Namatame H, Fugimori A, Yoshihara H, Ohtani T, Misu A and Takano M 1994 *Phys. Rev.* B **49** 16 191
[4] Vandenberg J M and Brasen D 1980 *J. Solid State Chem.* **35** 50
[5] Sahoo Y and Rastogi A K 1995 *Physica* B **215** 233
[6] Weigers G A 1980 *Physica* B **99** 151
[7] Gronvold F, Haraldsen H, Pedersen B and Tufte T 1969 *Rev. Chim. Miner.* **6** 215
De Vries A B and Jellinek F 1974 *Rev. Chim. Miner.* **11** 624
[8] Henderson L L and Goodenough J B 1995 *J. Solid State Chem.* **114** 346
[9] van Bruggen C F and Haas C 1976 *Solid State Commun.* **20** 251
[10] Kawada I, Nakano-Onada M, Ishii M, Saeki M and Nakahira M 1975 *J. Solid State Chem.* **15** 246
[11] Nozaki H, Ishizawa Y and Saeki M 1975 *Phys. Lett.* A **54** 29
[12] Forsyth J B, Brown P J, Kawada I, Nazaki H and Saeki M 1979 *J. Phys. C: Solid State Phys.* **12** 4261
[13] Silbernagel B J, Levy R and Gamble F R 1975 *Phys. Rev.* B **11** 4563
[14] Knect M, Ebert H and Bensch W 1998 *J. Phys.: Condens. Matter* **10** 9455
[15] Bensch W and Koy J 1993 *Inorg. Chim. Acta* **206** 221
[16] Nakano-Onada M, Yamaoka S, Yukino K, Kato K and Kamada I 1976 *J. Less-Common Met.* **44** 341
[17] Nakazawa H, Saeki M and Nakahira M 1975 *J. Less-Common Met.* **40** 57
[18] Jellinek F 1963 *Ark. Kemi* **20** 447
[19] Van Bruggen C F, Bloembergen J R, Bos-Alberink A J A and Weigers G A 1978 *J. Less-Common Met.* **60** 259
[20] Mutka H and Molini P 1982 *J. Phys. C: Solid State Phys.* **15** 6305
[21] Altshuler B L and Aronov A G 1985 *Electron–Electron Interaction in Disordered Systems* ed A L Efros and M Pollak (Amsterdam: Elsevier Science)
[22] Niazi A and Rastogi A K 2001 *J. Phys.: Condens. Matter* **13** 6787
[23] Wilson J A, DiSalvo F J and Mahajan S 1975 *Adv. Phys.* **24** 117
[24] Myron H W 1980 *Physica* B **99** 243
[25] Kitaoka Y and Yasuoka H 1980 *J. Phys. Soc. Japan* **48** 1949